

Sorption Sites, Energetics, and Reactions of Molybdenum Hexacarbonyl and Benzene Cosorbed in Faujasitic Zeolites

Claude Brémard,* Gabrielle Ginestet, and Marielle Le Maire

Contribution from the Laboratoire de Spectrochimie infrarouge et Raman, UPR-CNRS 2631, Bât. C5, Université des Sciences et Technologies de Lille, 59655 Villeneuve d'Ascq Cedex, France

Received April 4, 1996[⊗]

Abstract: Molecular simulations of the siting locations and energetics of Mo(CO)₆ and C₆H₆ cosorbed in faujasitic zeolites Na_nFAU (*n* = 0–96, Si/Al = 100–1) have been presented in combination with Diffuse Reflectance Infrared Fourier Transform Spectroscopy (DRIFTS). The *in situ* DRIFTS technique was found to be an efficient tool to monitor the cosorption at low coverage as well as the reaction of Mo(CO)₆ and C₆H₆ under thermal activation within the void space of the Na_nFAU zeolites. The molecular simulations are based on Monte Carlo calculations using the grand Canonical ensemble and are derived from a suitable zeolite-metal carbonyl-hydrocarbon potential set. From the present experimental and theoretical results as well as earlier experiments related to the reagents sorbed alone, a coherent picture of the cosorption and chemical behavior of Mo(CO)₆ and C₆H₆ within the void space of the faujasitic zeolites has been drawn as a function of the aluminum content. In siliceous faujasite (Si/Al = 100) the Mo(CO)₆ and C₆H₆ molecules are randomly distributed within the void space and the molecular motions approach the rapid isotropic limits of liquids. The chemical behavior upon thermal activation is found to be analogous to that observed in solution. In Na₅₆FAU (Si/Al = 2.5) the reagents are trapped in well-defined sorption sites in close proximity. Upon gentle thermal activation a fast reaction occurs to form Mo(CO)₃(η⁶-C₆H₆) inside the supercage through a concerted mechanism including the electrostatic field and the basicity of the framework oxygens. In Na_(85–96)FAU (Si/Al = 1.25, 1) the Mo(CO)₆ and C₆H₆ molecules are not encapsulated in close proximity. Mo(CO)₆ reacts thermally in the void space like in the absence of added C₆H₆ to lose sequentially three CO ligands and form predominantly a Mo(CO)₃(O₂)₃ species in which the three vacant coordination sites are occupied by three O₂ framework oxygens.

Introduction

Metal carbonyls supported on inorganic matrices can provide efficient catalytic systems.^{1–3} In particular, zeolites offer an advantage over many of the other supports such as alumina or silica in that the regular arrangement of pores helps to establish the binding sites for the metal carbonyl species.^{4–7} In this regard, the principal role of the zeolite is to immobilize the carbonyl species within the pores and to impart selectivity to a catalytic reaction by forcing the substrate molecule to pass through the zeolite channels to find the active species. Thus, only molecules of a certain size and shape will be able to participate in the catalytic reaction.

The group VI carbonyl metals engaged in faujasitic zeolites have been demonstrated to show catalytic activities for the metathesis of olefins^{1–4} as well as highly efficient and stereoselective activities for the isomerization and hydrogenation of dienes.^{8,9} The catalytically active species has been proposed to be a subcarbonyl species M(CO)₃ stabilized in the zeolitic framework. In addition, transient tricarbonyl diene complexes have been proposed as intermediates in the catalytic processes. The faujasitic zeolites, abbreviated hereafter as Na_nFAU, are

porous crystalline aluminosilicates with silicon aluminum ratios (Si/Al) in the [1–100] range. The M(CO)₆ molecules (M = Cr, Mo, W) have diameters in the range 7.4–7.6 Å and can therefore gain free access to the 13-Å diameter supercage through the 8-Å diameter 12-ring entrance port of faujasitic zeolites.

In an effort to provide a new insight into the intrazeolite organometallic chemistry,^{10–14} we have chosen to study here, a clean organo metallic reaction inside the void space of faujasitic zeolites. In choosing the archetypical reaction between Mo(CO)₆ and benzene, the following criteria should be satisfied: (i) the reaction has been well studied in homogeneous solutions;¹⁵ (ii) the intrazeolite benzene is structurally and spectroscopically well documented in FAU, Na₅₆FAU, and Na₈₅FAU,^{16–19} respectively. In addition, the mobility of benzene in FAU and Na₅₆FAU has been recently studied by molecular dynamics calculations;^{20–24} (iii) pertinent knowledge

[⊗] Abstract published in *Advance ACS Abstracts*, December 1, 1996.

(1) Bailey, D. C.; Langer, S. H. *Chem. Rev.* **1981**, *81*, 109.
 (2) Maxwell, J. E. *Adv. Catal.* **1982**, *31*, 1.
 (3) Gates, B. C.; Guzzi, L.; Knözinger, H. *Metal Clusters in Catalysis*; Elsevier: Amsterdam, 1986.
 (4) Ozin, G. A.; Gil, C. J. *Chem. Rev.* **1989**, *89*, 1749 and references cited therein.
 (5) Ozin, G. A.; Kuperman, A.; Stein, A. *Adv. Mater.* **1989**, *101*, 373.
 (6) Stucky, G. D.; MacDougall, J. *Science* **1990**, *247*, 669 and references cited therein.
 (7) Ozin, G. A.; Steele, M. R.; Holmes, A. J. *Chem. Mater.* **1994**, *6*, 999.
 (8) Okamoto, Y.; Kane, H.; Imanaka, T. *Catal. Lett.* **1989**, *2*, 335.
 (9) Okamoto, Y.; Onimatsu, H.; Hori, M.; Inui, I.; Imanaka, T. *Catal. Lett.* **1992**, *12*, 239.

(10) Schneider, R. L.; Howe, R. F.; Watters, K. L. *Inorg. Chem.* **1988**, *27*, 4030.

(11) Connaway, M. C.; Hanson, B. E. *Inorg. Chem.* **1986**, *25*, 1445.
 (12) Ozin, G. A.; Özkaz, S. *Chem. Mater.* **1992**, *4*, 511.
 (13) Li, X.; Ozin, G. A.; Özkaz, S. *J. Phys. Chem.* **1991**, *95*, 4463.
 (14) Ozin, G. A.; Haddleton, D. M.; Gil, C. J. *J. Phys. Chem.* **1989**, *93*, 6710.
 (15) Werner, R. P. M.; Coffield, T. H. *Chem. Ind.* **1960**, 936.
 (16) Fitch, A. N.; Jobic, H.; Renouprez, A. *J. Phys. Chem.* **1986**, *90*, 1311.
 (17) De Mallmann, A.; Barthomeuf, D. *Zeolites* **1988**, *8*, 292.
 (18) De Mallmann, A.; Barthomeuf, D. *J. Phys. Chem.* **1989**, *93*, 5636.
 (19) Coughlan, B.; Keane, M. A. *J. Chem. Soc., Faraday Trans.* **1990**, *86*, 3961.
 (20) Smit, B.; den Outen, C. J. J. *J. Phys. Chem.* **1988**, *92*, 7169.
 (21) Uytterhoeven, L.; Dompas, D.; Mortier, W. J. *J. Chem. Soc., Faraday Trans.* **1992**, *3*, 633.
 (22) Demontis, P.; Yashonath, S.; Klein, M. L. *J. Phys. Chem.* **1989**, *93*, 5016.
 (23) Auerbach, S. M.; Henson, N. J.; Cheetham, A. K.; Metiu, H. I. *J. Phys. Chem.* **1995**, *99*, 10600.

to the characterization of the intrazeolite Mo(CO)₆ and Mo(CO)₃ species as well as dynamic motions has been acquired to date.^{25–40}

Techniques utilized to date to investigate the metal carbonyl species encapsulated in zeolites include chemical techniques, IR, Raman, ESR, NMR, XPS, EXAFS spectroscopy. However, many of these techniques are particularly devoted to highly loaded samples. Now, to avoid the problem of pore blocking which can hinder the intracrystalline diffusion at high coverage, the cosorption experiments were carried out at Mo(CO)₆ low coverage. So, the Diffuse Reflectance Infrared Spectroscopy (DRIFTS) was found to be an efficient tool to monitor at low coverage, the loading, siting sites of C₆H₆, Mo(CO)₆ molecules and reaction products, at the different stages of the experiments (sorption, cosorption and reaction).^{36,41} In spite of the dynamic aspects through the zeolite lattice, the sorbates can be considered to exist at the time of the reaction in well defined sites or in random positions. The predictions of energetics and siting locations of sorbates from Monte Carlo simulations are expected to provide pertinent information in this field.

We present here Monte Carlo simulations and Diffuse Reflectance Infrared (DRIFTS) investigations of the cosorption of Mo(CO)₆ and benzene in faujasitic zeolites Na_nFAU (*n* = 0, 56, 85, 96) as well as subsequent reactions. Some aspects of the stoichiometry of the intrazeolite reaction have been reported earlier⁴¹ and a detailed quantitative kinetic study of Mo(¹²CO)₆ with ¹³CO or trimethyl phosphine encapsulated in Na₅₆FAU has been recently published.⁴² The first purpose of the present work is to provide information about the molecular organization and the cooperative effects between the sorbates within the different zeolites at room temperature as functions of the loadings of the sorbates as well as a function of the Si/Al ratio of the zeolite; the second one is the *in situ* study of the reaction under thermal activation including the identification of the products, the stoichiometry, and some qualitative kinetic aspects of the

reaction; the last one is to provide information about the molecular organization of the reaction products within the zeolite framework.

Experimental Section

Materials. The completely siliceous FAU zeolite (Si/Al > 100) was kindly provided by Degussa. The Na₅₆FAU zeolite (Si/Al = 2.49) was obtained from Union Carbide. The Na₈₅FAU (Si/Al = 1.26) and Na₉₆FAU zeolites (Si/Al = 1) were kindly provided by J. L. Reymonet (CECA). The average crystallite size of all the zeolite samples is approximately 0.5 μm and an average particle size is 5 μm.

Mo(CO)₆ and C₆H₆ were purchased from Strem Chemicals Inc and used after dehydration. Mo(CO)₃(η⁶-C₆H₆) was prepared as previously described.^{15,43}

Techniques. The FTIR spectrometer was a Bruker IFS 113 V instrument equipped with a liquid nitrogen cooled MCT detector (mid-IR) with the suitable beam splitter. The opus Bruker software was used for spectral acquisition, storage, manipulation, and plotting. The spectra were recorded at 2 cm⁻¹ resolution.

The key part of the *in situ* DRIFTS apparatus is a modified version of a Harrick Scientific Diffused Reflectance Attachment << DRA-2CI >> Praying mantis and << HVC-DRP >> cell equipped with CaF₂ windows operating from 100 K to 800 K. The volume of powder viewed by the DRIFTS technique corresponds approximately to a disc of 4 mm in diameter and 1 mm in depth.⁴⁴ This particularity is very efficient to study the sorption at very low coverage.³⁷ Conventionally, an equation derived from the Kubelka-Munk phenomenological theory⁴⁵ is used in order to relate a chromophore concentration of the intensity of the sample diffuse reflection. In this equation: $F(R) = (1-R)^2/2R = K/S$, the sample is treated as a continuum, *R* represents the ratio of the diffuse reflectance of the loaded zeolite to that of the dehydrated neat zeolite, and *K* designates an absorption coefficient proportional to the concentration *C* of the chromophore and *S* the scattering coefficient of the powder.

The crystallinity and the purity of the dehydrated and loaded samples were checked by X-ray powder diffraction patterns (XRD). The elemental analyses for Na, Al, Mo were obtained using the ICP technique.

The modeling results published herewith were generated using the program Cerius² developed by Molecular Simulations Incorporated.

Cosorption and Reaction of Mo(CO)₆ and C₆H₆ in Zeolites. Upstream of the DRIFTS cell are vacuum and gas lines (He, O₂) and a reaction delivery system.^{36,41} The dehydrated solid Mo(CO)₆, dehydrated liquid C₆H₆ were stocked in bypass systems under argon. The sequence of steps in a typical adsorption experiment was as follows: the powdered zeolite sample is introduced into the cell connected to the vacuum line. The sample is pumped down to a pressure of 10⁻³ Pa and heated stepwise to 700 K, and then O₂ gas is admitted into the cell. After 6 h, the sample is pumped down to a pressure of 10⁻³ Pa and then cooled to room temperature. Dry He carrier gas is drawn through the dehydrated zeolite. A reference spectrum of the neat zeolite is run subsequently. A side arm containing Mo(CO)₆ or C₆H₆ is opened for different periods and spectra are recorded after each period during and after the equilibrium phase at different temperatures. At low coverage, the equilibrium period of the loaded FAU zeolites (Si/Al < 2.5) was estimated to be 24 h under He at room temperature. This period can be reduced under gentle warming. Unfortunately, it should be noted that the decomposition of Mo(CO)₆ occurs in FAU zeolites (Si/Al > 2.5) some hours after the loading at room temperature. So, the cosorption of Mo(CO)₆ and C₆H₆ was carried out at 273 K before the thermal activation. At low coverage, the loadings of Mo(CO)₆, C₆H₆ were obtained through the infrared intensity using the Kubelka-Munk scale $F(R) = (1-R)^2/2R = K/S$ which is assumed to be proportional to the concentration. The calibration was obtained by taking as standard three higher zeolites loaded with Mo(CO)₆ or C₆H₆, respectively.

Sorption of Mo(CO)₃(η⁶-C₆H₆) in Zeolites. A pentane solution of Mo(CO)₃(η⁶-C₆H₆) was added under argon by syringe to an activated

(24) Bull, L. M.; Henson, N. J.; Cheetham, A. K.; Newsam, J. M.; Heyes, S. J. *J. Phys. Chem.* **1993**, *97*, 11776.

(25) Coudurier, G.; Gallezot, H.; Praliaud, H.; Primet, M.; Imelik, B. C. *R. Acad. Sci. Paris C* **1976**, *282*, 311.

(26) Bein, T.; Jacobs, P. A. *J. Chem. Soc., Faraday Trans.* **1983**, *79*, 1919.

(27) You-sing, Y.; Howe, R. F. *J. Chem. Soc., Faraday Trans. I* **1986**, *82*, 2887.

(28) Özkar, S.; Ozin, G. A.; Moller, K.; Bein, T. *J. Am. Chem. Soc.* **1990**, *112*, 9575 and references cited therein.

(29) Zecchina, A.; Bordiga, S.; Escalona Platero, E.; Otero Arean, C. J. *Catal.* **1990**, *125*, 568.

(30) Borvornwattananont, A.; Moller, K.; Bein, T. *J. Phys. Chem.* **1989**, *93*, 4205.

(31) Ozin, G. A.; Özkar, S.; Macdonald, P. *J. Phys. Chem.* **1990**, *94*, 6939.

(32) Moller, K.; Bein, T.; Özkar, S.; Ozin, G. A. *J. Phys. Chem.* **1991**, *95*, 5276.

(33) Jelinek, R.; Özkar, S.; Pastore, H. O.; Malek, A.; Ozin, G. A. *J. Am. Chem. Soc.* **1993**, *115*, 563.

(34) Okamoto, Y.; Maezawa, A.; Kane, H.; Imanaka, T. *J. Chem. Soc., Faraday Trans. I* **1989**, *84*, 851.

(35) Okamoto, Y.; Imanaka, T.; Asakura, K.; Iwasawa, Y. *J. Phys. Chem.* **1991**, *95*, 3700 and references cited therein.

(36) Brémard, C.; Depecker, C.; Des Grouilliers, H.; Legrand, P. *Appl. Spectrosc.* **1991**, *45*, 1278.

(37) Brémard, C.; Ginestet, G.; Laureyns, J.; Le Maire, M. *J. Am. Chem. Soc.* **1995**, *117*, 9274 and references cited therein.

(38) Wagner, G. W.; Hanson, B. E. *J. Am. Chem. Soc.* **1989**, *111*, 5098.

(39) Shirley, W. M.; Powers, C. A.; Tway, C. L. *Coll. Surf.* **1990**, *45*, 57.

(40) Cybulski, P. A.; Gillis, D. J.; Baird, M. C. *Inorg. Chem.* **1993**, *32*, 460.

(41) Brémard, C.; Des Grouilliers, H.; Depecker, C.; Legrand, P. *J. Chem. Soc., Chem. Commun.* **1991**, 1411.

(42) Pastore, O. H.; Ozin, G. A.; Poë, A. J. *J. Am. Chem. Soc.* **1993**, *115*, 1215.

(43) Wagner, G. W.; Hanson, B. E. *Inorg. Chem.* **1987**, *26*, 2019.

(44) Fraser, D. J. J.; Griffiths, P. R. *Appl. Spectroscop.* **1990**, *44*, 193.

(45) Kubelka, P.; Munk, F. *Z. Tech. Phys.* **1931**, *12*, 593.

zeolite sample. The zeolite was loaded with $\text{Mo}(\text{CO})_3(\eta^6\text{-C}_6\text{H}_6)$ by immersion into the pentane solution. The powder was collected by filtration under argon and dried under vacuum and then transferred into the DRIFTS cell in a glovebox.

Theoretical Methods. The atomic positions for the zeolite hosts, FAU, Na_{56}FAU , and Na_{85}FAU , were obtained from all the available X-ray or neutron diffraction determinations of the structures.^{16,21,46–48} In the simulations the silicon, aluminum, oxygen atoms of the zeolite framework and extraframework cations are assumed to be fixed at the crystallographic coordinates determined from structural data. The substitutional Si, Al disorder was applied according to the Lowenstein rule. The partial occupancy of extraframework cation sites was taken into account explicitly in view of the extensive structural work published in the literature.^{47,48} From X-ray powder diffraction studies Van Dun *et al.* concluded that the influence of adsorbed molecules on the cation distribution increases with the cation-molecule interaction energy.⁴⁹ In the case of the adsorption of hydrophobic molecules such as benzene the extraframework cation moving was found negligible. Fitch *et al.* reported a shift of 0.009 nm of Na^+ cations in Na_{56}FAU due to the interaction of benzene.¹⁶ The interaction of intrazeolite $\text{Mo}(\text{CO})_6$ with rubidium cations of the zeolite has been probed previously with rubidium edge EXAFS data.²⁸ The data of the empty rubidium exchanged zeolite as well as the $\text{Mo}(\text{CO})_6$ loaded sample were found to be very similar. The error made by fixing the cation positions throughout the calculations is therefore assumed negligible.²³ For these reasons, the zeolite structure including Na ions is held rigid and fixed for the calculations. $\text{Mo}(\text{CO})_6$, $\text{Mo}(\text{CO})_3$, $\text{Mo}(\text{CO})_3(\eta^6\text{-C}_6\text{H}_6)$, and C_6H_6 are modeled as rigid molecules. The geometrical parameters of the sorbates $\text{Mo}(\text{CO})_6$, $\text{Mo}(\text{CO})_3$, $\text{Mo}(\text{CO})_3(\eta^6\text{-C}_6\text{H}_6)$, and C_6H_6 are obtained from electronic diffraction data⁵⁰ or optimized geometry using *ab initio* method⁵¹ or deduced from X-ray diffraction^{52–54} or EXAFS data.^{12,28,35} In addition the weak deformations of the guest molecule skeleton which occur upon sorption are assumed to be negligible according to previous EXAFS^{28,35} and neutron diffraction results, respectively.¹⁶

The zeolite (Z) and the sorbates (S) are assumed to interact through pairwise-additive potential between atoms of the guests and atoms of the host (U_{ZS}). For simulations at higher loadings, the interactions between sorbates (U_{SS}) must also be included. The atom–atom interactions are modeled with a Lennard-Jones plus point-charge potential,

$$U_{ZS} = \sum_{ij} A_{ij}/n_j^{12} - B_{ij}/n_j^6 + \sum_{ij} q_i q_j / r_{ij} \quad (1)$$

$$U_{SS} = \sum_{ik} A_{ik}/r_{ik}^{12} - B_{ik}/r_{ik}^6 + \sum_{jk} q_j q_k / r_{jk} \quad (2)$$

where i and j,k are atoms of the Na_nFAU (Z) host and (S) guests, respectively, and r_{ij} and r_{jk} are the distances between them. A , B are the Lennard-Jones constants and q is the partial charges of the atoms. The Lennard-Jones potential accounts for dispersive and repulsive interactions and the values used throughout the present work were taken from the literature^{20,22–24,37,55–58} and are listed in Table 1 as A_{ij} and B_{ij} parameters, where $A_{ij} = (A_i A_j)^{1/2}$ and $B_{ij} = (B_i B_j)^{1/2}$.

(46) Hriljac, J. A.; Eddy, M. M.; Cheetham, A. K.; Donohue, J. A.; Ray, G. J. *J. Solid State Chem.* **1993**, *106*, 66.

(47) Lievens, J. L.; Mortier, W. J.; Chao, K. J. *J. Phys. Chem. Solids* **1992**, *53*, 1163.

(48) Mortier, W. J. *Compilation of Extra-framework Sites in Zeolites*; issued by the Commission of the International Zeolite Association, 1981.

(49) Van Dun, J. J. L.; Mortier, W. J.; Uytterhoeven, J. B. *Zeolites* **1985**, *5*, 257.

(50) Arnesen, S. P.; Seip, H. M. *Acta Chim. Scand.* **1966**, *20*, 2711.

(51) Li, J.; Schreckenbach, G.; Ziegler, T. *J. Phys. Chem.* **1994**, *98*, 4838 and publications cited therein.

(52) Jost, A.; Rees, B. *Acta Crystallogr.* **1975**, *B 31*, 2647.

(53) Whitaker, A.; Jeffery, J. W. *Acta Crystallogr.* **1967**, *23*, 977.

(54) Rees, B.; Coppens, P. *Acta Cryst.* **1973**, *B29*, 2515.

(55) Brubaker, G. R.; Johnson, D. W. *Coord. Chem. Rev.* **1984**, *53*, 1.

(56) Kiselev, A. V.; Lopatkin, A. A.; Shulga, A. A. *Zeolites* **1985**, *5*, 261.

(57) Besus, A. G.; Kocirik, M.; Kiselev, A. V.; Lopatkin, A. A.; Vasilyeva, E. A. *Zeolites* **1986**, *6*, 101.

(58) Yashonath, S.; Santikary, P. *J. Phys. Chem.* **1994**, *98*, 6368.

Table 1. Summary of the Potential Parameters and Atomic Charges Used To Represent the Zeolite–Sorbate Interactions

atom	charge (e)	A (kcal mol ⁻¹ Å ¹²)	B (kcal mol ⁻¹ Å ⁶)
Si (FAU)	1.5	1.720×10^6	0.0
O (FAU)	-0.75	1.806×10^5	821
Si (Na_{56}FAU)	1.42	1.720×10^6	0.0
Al (Na_{56}FAU)	1.23	1.720×10^6	0.0
O (Na_{56}FAU)	-0.83	1.806×10^5	821
Si (Na_{96}FAU)	1.35	1.720×10^6	0.0
Al (Na_{96}FAU)	1.13	1.720×10^6	0.0
O (Na_{96}FAU)	-0.87	1.806×10^5	821
Na^+	1	1.289×10^6	55
Mo ($\text{Mo}(\text{CO})_6$)	0.06	0.0	0.0
O (CO)	-0.21	1.316×10^5	103
C (CO)	0.20	1.975×10^5	154
Mo ($\text{Mo}(\text{CO})_3$)	0.03	1.921×10^5	12
C (C_6H_6)	-0.15	2.202×10^5	240
H (C_6H_6)	0.15	7.108×10^3	33

The charge distribution within FAU-type structures are derived from the ref 21. They suggest that the concept of localized partial charge can be used efficiently to reproduce the electrostatic field with a correct approximation in the present system. The charge estimates of $\text{Mo}(\text{CO})_6$ and C_6H_6 are derived from quantum chemical population analysis.^{23,59,60} The localized atomic charges of $\text{Mo}(\text{CO})_3$ and $\text{Mo}(\text{CO})_3(\eta^6\text{-C}_6\text{H}_6)$ were estimated. We would like to point out that the polarizability interactions between the sorbate and zeolite atoms are not taken into account explicitly. This is expected to contribute not more than 10% to the total interaction. We believe that the results and in particular the trends reported here will remain unchanged on the inclusion of the polarizability interactions. The sorption sites and energetics of C_6H_6 in Na_{56}FAU are well reproduced with the set of atom-atom potentials and partial charges used throughout the present paper.

The Monte Carlo simulations at fixed loading (1 sorbate per unit cell) were carried out at 300 K using the conventional Metropolis algorithm. This allows us to ignore sorbate–sorbate interactions. One molecule is initially placed inside a micropore of the zeolite. One Monte Carlo step consists of a random displacement of the center of mass followed by an arbitrary rotation of the entire molecule. In order to eliminate the effect of boundaries we have used periodic boundary conditions with a period equal to one zeolite unit cell. A cutoff radius of 12 Å is applied to the Lennard-Jones interactions and the long-range electrostatic interactions are calculated using the Ewald summation technique. Each configuration is accepted or rejected using a Metropolis algorithm based on the configurational energy change: $P = \min [1; \exp(-\Delta E/kT)]$ where P probability of the move being accepted, ΔE energy change between the new configuration and the previous configuration, k Boltzmann's constant, and T temperature of the simulation. One typical MC run took 1 000 000 steps.

The Monte Carlo simulations of the sorption and cosorption at fixed pressures were carried out using the grand canonical ensemble (GCMC); in this the number of particles in the system is determined by the fixed chemical potential of each species. One Monte Carlo step consists of four parts (create, destroy, translate, and rotate a molecule). The basis of the simulation is as follows.

Equilibrium is achieved when the temperature and the chemical potential of the gas inside the framework are equal to the temperature and the chemical potential of the free gas outside the framework.

A random molecule is picked from the list of sorbates, and placed in a random position and orientation in the framework. The new configuration is accepted with probability $P:P = \min [1; \exp(-\Delta E/kT - \ln(N_i + 1)kT/f_iV)]$ where P , ΔE , k , and T were defined above, N_i is the current number of molecules of component i in framework, f_i is

(59) Kunze, K. L.; Davidson, E. R. *J. Phys. Chem.* **1992**, *96*, 2129.

(60) Bauschlicher Jr, C. W.; Bagus, P. S. *J. Phys. Chem.* **1984**, *81*, 5889.

(61) Folkesson, B.; Larsson, R. *J. Electron. Spectrosc. Relat. Phenom.* **1990**, *81*, 5889.

(62) Hriljac, J. A.; Eddy, M. M.; Cheetham, A. K.; Donohue, J. A.; Ray, G. J. *J. Solid State Chem.* **1993**, *76*, 145.

(63) Howell, J. A. S.; Ashford, N. F.; Dixon, D. T.; Kola, J. C.; Albright, T. A.; Kang, S. K. *Organometallics* **1991**, *10*, 1852.

the fugacity of component *i* in the gas phase assumed to be 1, and *V* is cell volume.

The simulation randomly chooses which sorbate type to remove, then randomly chooses a molecule of that type in the framework. The new configuration is accepted with probability $P:P = \min[1; \exp(-\Delta E/kT + \ln N_i/kT/f_i V)]$. A sorbate molecule in the framework is chosen at random, and translated by a random amount within a cube of size 2δ (where δ is the maximum step size). The new configuration is accepted with the probability *P*. The acceptance criterion is the same as for the fixed loading simulation (see above).

A sorbate molecule in the framework is chosen in the framework. The rotation axis is chosen at random, and the molecule is rotated by a random amount within the range $-\delta$ to $+\delta$ (where δ is the maximum step size). The new configuration, based on the energy change, is accepted with the same probability applied to the translation move above. The simulation takes a number of steps to equilibrate from its original random position. For accurate statistical results, the steps made prior to equilibration should be excluded in the analysis. One typical GCMC run took from 2 000 000 to 3 000 000 steps.

Results and Discussion

Dynamic and Cooperative Effects within the Zeolitic Void Space. DRIFTS Investigations of the Cosorption of Mo(CO)₆ and C₆H₆ into Na_{*n*}FAU Zeolite Hosts (*n* = 0, 56, 85, 96). The DRIFTS technique allows the use of crude powders as samples, so the molecules can diffuse easily in the intercrystalline void space. However, in order to avoid the problem of pore blocking which can hinder the intracrystalline diffusion at high coverage in zeolites, the cosorption DRIFTS experiments were carried out at Mo(CO)₆ low coverage. The DRIFTS technique is particularly sensitive to the presence of carbonyl species at very low loading (see Experimental Section) and provides valuable information through the $\nu(\text{CO})$ stretching modes of the *in situ* investigations of the cosorption and subsequent reaction in the zeolitic porous materials. Mo(CO)₆ and benzene were introduced into the system via two differentially pumped gas inlet manifolds. Firstly, the zeolite host was loaded with Mo(CO)₆ by exposing the dehydrated zeolite (273 K) to the vapor pressure of Mo(CO)₆ for a short period. After an equilibrium period the DRIFTS spectrum was recorded and the coverage was deduced through the infrared intensities using the Kubelka-Munk scale (see Experimental Section). Then, the C₆H₆ was admitted into the cell and the DRIFTS spectra run subsequently after an equilibrium period. In order to provide supplementary evidence of the free access of both Mo(CO)₆ and C₆H₆ in the internal voids of the porous materials under study through the 12-ring entrance window, size exclusion studies were carried out. The use of bulky arenes, such as 1,3,6-tris(*tert*-butyl)benzene, C₆H₃(*t*-Bu)₃, and small arenes such as C₆H₆ demonstrates the exclusive free access to the internal surface for the small arene, C₆H₆, with analogous experimental conditions. C₆H₃(*t*-Bu)₃ is effectively size-excluded from the porous voids. One concludes from the present and previous articles²⁸ that the DRIFTS investigations of the benzene-Mo(CO)₆ cosorption are representative of the internal confines of the zeolite host lattice and not of the external surface of the microcrystals.

FAU (*n* = 0; Si/Al > 100). The sorption of Mo(CO)₆ (0.1–0.5 Mo(CO)₆/unit cell) into the siliceous FAU undergoes the isotropic perturbation of the O_h symmetry of the isolated Mo(CO)₆ molecule which results in weak band broadening of the $\nu_6(\text{F}_{1u})$ infrared active mode, Figure 1. The similarity between the IR spectra of Mo(CO)₆ in solution and occluded in the siliceous FAU provides evidence that the motion of the Mo(CO)₆ molecule within the porous voids approaches at room temperature the rapid isotropic limit characteristic of a liquid.³⁷

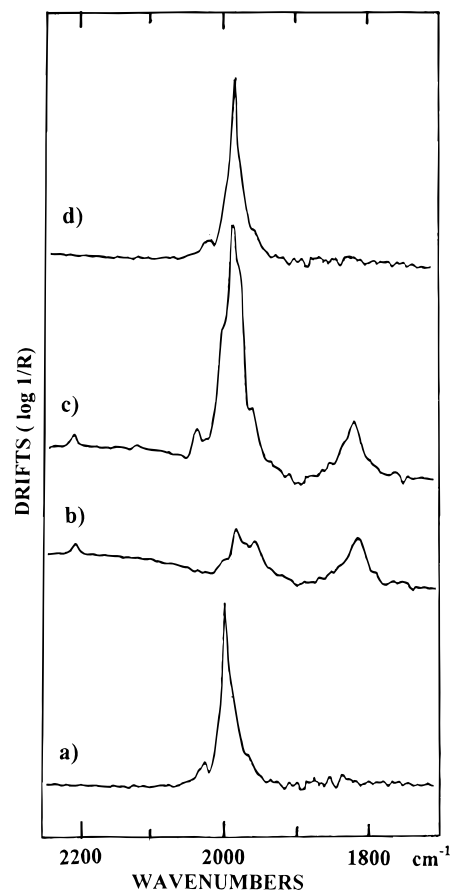


Figure 1. DRIFTS spectra (300 K) in the $\nu(\text{CO})$ fundamental and $\gamma(\text{C-H})$ combination modes region of (a) Mo(CO)₆ sorbed in FAU (0.2 Mo(CO)₆/unit cell); (b) C₆H₆ sorbed in FAU (20 C₆H₆/unit cell); (c) Mo(CO)₆ and C₆H₆ cosorbed in FAU (0.2 Mo(CO)₆, 20 C₆H₆/unit cell); (d) c spectrum after subtraction of the b C₆H₆ spectrum (20 C₆H₆/unit cell).

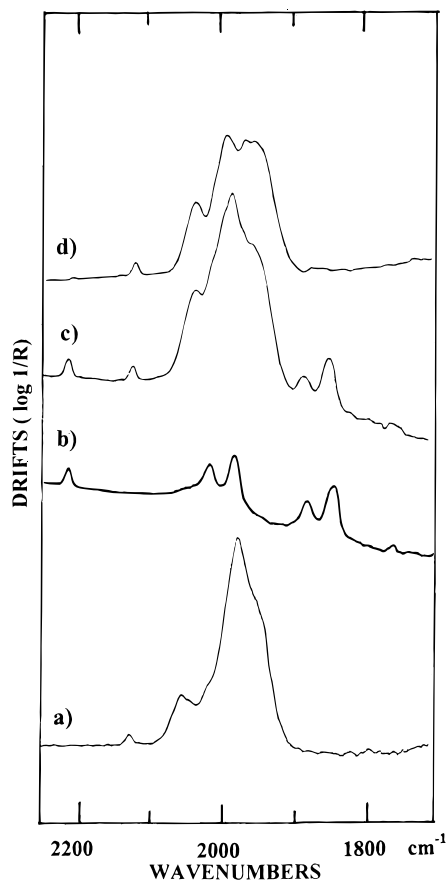
Upon sorption of C₆H₆ (15–30 C₆H₆/unit cell) in the presence of Mo(CO)₆ (0.1–0.5 Mo(CO)₆/unit cell) additional bands are observed in the wavenumber ranges of the vibrational modes of benzene. Particularly, the bands at 2208, 1960, 1815 cm⁻¹ are exhibited in the Figure 1. The similarity between the IR spectra of C₆H₆ in solution, sorbed and cosorbed in FAU provides evidence that the C₆H₆ molecules within the porous voids approach, at room temperature, the rapid limit characteristic of liquid. Upon sorption in FAU the IR spectrum of benzene hardly changes as the benzene loading increases.

According to previous experiments,^{17–19} the bands observed at 1960 and 1820 cm⁻¹ (Figure 1) are assigned to combination modes of out-of-plane bending modes $\gamma(\text{C-H})$ whereas the intense band at 1478 cm⁻¹ is assigned to the fundamental $\nu_{19}(\text{E}_{1u})$ stretching mode $\nu(\text{C-C})$. After subtraction from the cosorbed sample spectrum of the spectrum of benzene sorbed alone, the remaining one band spectrum is found to be analogous to the spectrum of Mo(CO)₆ sorbed alone in the FAU zeolite, except for a weak frequency shift. A random distribution of both the Mo(CO)₆ and benzene molecules within the porous void of siliceous FAU is postulated subsequently.

Na₅₆FAU (*n* = 56; Si/Al = 2.49). The DRIFTS spectrum of Mo(CO)₆ sorbed into the Na₅₆FAU zeolite at low coverage (0.1–0.5 Mo(CO)₆/unit cell) exhibits after equilibration a $\nu(\text{CO})$ absorption pattern which is characteristic of a well-defined adsorption site with low local symmetry, Figure 2. This adsorption site has been found to be in a 12-ring window of a supercage.³⁷ The intracavity electrostatic field promotes the breakdown of the selection rules of the free molecule and

Table 2. DRIFTS ν^a (CO) Frequencies (cm^{-1}) of Carbonyl Molybdenum Species Sorbed and Cosorbed with Benzene in Na_nFAU Zeolites ($n = 0, 56, 85$)

carbonyl species	FAU	FAU C_6H_6	Na_{56}FAU	$\text{Na}_{56}\text{FAU C}_6\text{H}_6$	Na_{85}FAU	$\text{Na}_{85}\text{FAU C}_6\text{H}_6$
$\text{Mo}(\text{CO})_6$			2125	2125	2125	2125
			2060	2045	2050	2050
			2015	2000	2005	2005
	1990	1985	1980	1970	1985	1985
			1950	1955	1970	1970
			1930	1940	1945	1945
$\text{Mo}(\text{CO})_3$			1907		1902	1902
			1790		1775	1775
			1760		1750	1750
$\text{Mo}(\text{CO})_3(\eta^6\text{C}_6\text{H}_6)$	1930		1945	1948		
	1845		1860	1857		
			1830	1832		

^a Determined using spectral decomposition.**Figure 2.** DRIFTS spectra (300 K) in the $\nu(\text{CO})$ fundamental and $\gamma(\text{C-H})$ combination modes region of (a) $\text{Mo}(\text{CO})_6$ sorbed in Na_{56}FAU (0.3 $\text{Mo}(\text{CO})_6/\text{unit cell}$); (b) C_6H_6 sorbed in Na_{56}FAU (20 $\text{C}_6\text{H}_6/\text{unit cell}$); (c) $\text{Mo}(\text{CO})_6$ and C_6H_6 cosorbed in Na_{56}FAU (0.3 $\text{Mo}(\text{CO})_6$, 20 $\text{C}_6\text{H}_6/\text{unit cell}$); (d) c spectrum after subtraction of the b C_6H_6 spectrum (20 $\text{C}_6\text{H}_6/\text{unit cell}$).

induces the splitting of the $\nu_6(\text{F}_{1u})$ band into three components and the appearance and splitting of the $\nu_3(\text{E}_g)$ mode and the appearance of the $\nu_1(\text{A}_{1g})$ IR-forbidden modes of the free molecule, see Figure 2.

Upon adsorption of C_6H_6 (16–30 $\text{C}_6\text{H}_6/\text{unit cell}$) in the presence of $\text{Mo}(\text{CO})_6$ (0.1–0.5 $\text{Mo}(\text{CO})_6/\text{unit cell}$) additional bands are observed in the vibration regions of the C_6H_6 molecule. The bands observed at 2220, 1880, 1847 cm^{-1} (Figure 2) as other bands are in correct agreement with previously reported data concerning benzene sorbed alone in Na_{56}FAU zeolite.¹⁸ Particularly, the shape of the bands progressively changes as the benzene loading increases. The two pairs of IR bands 2013, 1880, and 1983, 1847 cm^{-1} corresponding to the out-of-plane $\gamma(\text{C-H})$ combination modes

were used previously to characterize the benzene adsorption sites.¹⁸ According to neutron diffraction data, the dominant site lies in the supercage, facially coordinated to the SII Na^+ cation and the second is centered in the 12-ring window.¹⁶ The high-frequency pair 2013, 1880 cm^{-1} is related to the benzene sorbed in the 12-ring window whereas the lower-frequency pair 1983, 1847 cm^{-1} arises from benzene with the Na^+ cations in sites II.¹⁸ The preference for SII Na^+ cations mentioned above is detected at low C_6H_6 loadings, the adsorption in the 12-ring window starting to increase significantly only after 20 C_6H_6 per unit cell are sorbed. It should be noted that other cationic faujasites may give a different order of preferred adsorption.¹⁸ After subtraction from the DRIFTS pattern (cosorbed samples) of the spectrum of benzene (singly sorbed sample) the remaining spectrum does not correspond to the spectrum of $\text{Mo}(\text{CO})_6$ sorbed alone in the Na_{56}FAU zeolite (Figure 2). The $\nu(\text{CO})$ wavenumber values obtained using spectral decomposition have been listed in Table 2. The DRIFTS spectra indicate significant frequency shifts and relative IR intensity changes of the $\nu(\text{CO})$ modes upon cosorption of benzene. It is postulated that the presence of benzene in the porous void generates a new sorption site for $\text{Mo}(\text{CO})_6$ with C_6H_6 molecules in close proximity.

$\text{Na}_{85-96}\text{FAU}$ ($n = 85$, $\text{Si}/\text{Al} = 1.26$; $n = 96$, $\text{Si}/\text{Al} = 1$). The DRIFTS spectrum of $\text{Mo}(\text{CO})_6$ sorbed into the Na_{85}FAU zeolite at low coverage (0.1–0.5 $\text{Mo}(\text{CO})_6/\text{unit cell}$) exhibits a six $\nu(\text{CO})$ absorption pattern which is characteristic of a well-defined adsorption site with low local symmetry, Figure 3. However, the occupancy of the SIII sites by Na^+ cations in the vicinity of the window constrains the $\text{Mo}(\text{CO})_6$ to penetrate inside the supercage at low coverage.³⁷

Upon sorption of C_6H_6 (16–30 $\text{C}_6\text{H}_6/\text{unit cell}$) in the presence of $\text{Mo}(\text{CO})_6$ (0.1–0.5 $\text{Mo}(\text{CO})_6/\text{unit cell}$) additional bands are clearly observed at 2220, 1866, 1847 cm^{-1} (Figure 3) as other bands in the fundamental vibration regions of the C_6H_6 molecule. The IR bands of C_6H_6 are found to be analogous to those observed previously for benzene sorbed alone in Na_{85}FAU . The pair of bands observed at 1866 and 1847 cm^{-1} is found to be typical of two types of adsorption sites for benzene.¹⁷ However, the distribution of benzene between the two modes of sorption, cations and 12-ring windows is strongly directed by the chemical properties of the zeolite. After subtraction from the DRIFTS pattern (cosorbed sample) of the DRIFTS spectrum of benzene (singly sorbed sample), the remaining $\nu(\text{CO})$ spectrum is found to be analogous to the spectrum of $\text{Mo}(\text{CO})_6$ sorbed alone in the Na_{85}FAU zeolite at 273 K (Figure 3). The $\nu(\text{CO})$ wavenumber values obtained using spectral decomposition have been listed in Table 2. The DRIFTS spectra indicate no significant frequency shifts and relative IR intensity changes of the $\nu(\text{CO})$ modes upon cosorption of benzene. It is

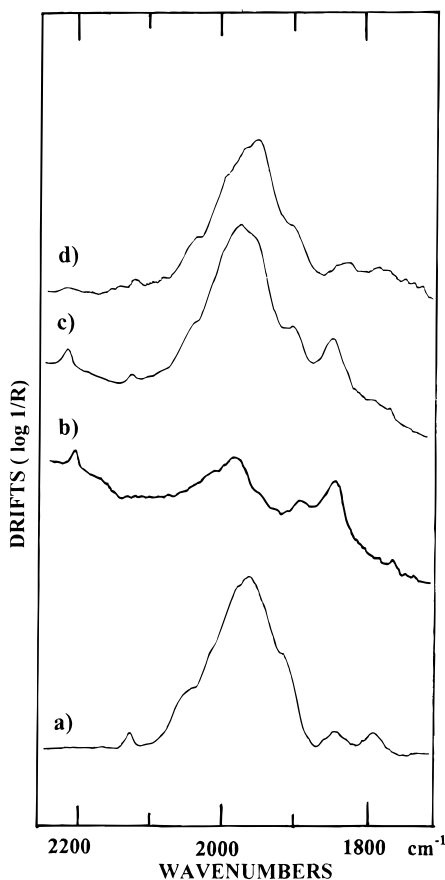


Figure 3. DRIFTS spectra (300 K) in the $\nu(\text{CO})$ fundamental and $\gamma(\text{C-H})$ combination modes region of (a) $\text{Mo}(\text{CO})_6$ sorbed in Na_{85}FAU (0.3 $\text{Mo}(\text{CO})_6$ /unit cell); (b) C_6H_6 sorbed in Na_{85}FAU (0.3 $\text{Mo}(\text{CO})_6$, 20 C_6H_6 /unit cell); (c) $\text{Mo}(\text{CO})_6$ and C_6H_6 cosorbed in Na_{85}FAU (0.3 $\text{Mo}(\text{CO})_6$, 20 C_6H_6 /unit cell); (d) c spectrum after subtraction of the b C_6H_6 spectrum (20 C_6H_6 /unit cell).

postulated that the sorptions of $\text{Mo}(\text{CO})_6$ and benzene occur in different domains of the porous void of Na_nFAU ($n = 85-96$).

Energetics and Sorption Sites of $\text{Mo}(\text{CO})_6$ and C_6H_6 in the Zeolitic Void Space. Monte Carlo Simulations of the Cosorption of $\text{Mo}(\text{CO})_6$ and C_6H_6 into Na_nFAU Zeolite Hosts ($n = 0, 56, 96$). The DRIFTS spectroscopic results are supported by Grand Canonical Monte Carlo (GCMC) simulations of the cosorption of $\text{Mo}(\text{CO})_6$ and C_6H_6 at constant pressures. The pressure values were adjusted to approximately mimic the experimental coverages. The conditions of the simulations have been given in the Experimental Section. The potential parameters and charges used for the MC simulations of the host-guest interactions are summarized in Table 1. The validity of the set of parameters used throughout the present article is given by the possibility to reasonably reproduce the experimental C_6H_6 loadings in Na_nFAU ($n = 0, 56, 96$)¹⁸ and the siting locations of C_6D_6 in Na_{56}FAU .^{16,23} In addition, the predicted $\text{Mo}(\text{CO})_6$ siting locations are in close agreement with the spectroscopic behavior of $\text{Mo}(\text{CO})_6$ occluded in Na_nFAU ($n = 0, 56, 85$).³⁷

FAU ($n = 0$). The prediction of cosorption was carried out at 300 K and the constant pressures were adjusted to correspond approximately to the respective experimental loadings. In the presence of C_6H_6 at high pressure, no $\text{Mo}(\text{CO})_6$ cosorption was simulated and all the porous volume is filled with C_6H_6 molecules (32 C_6H_6 /unit cell). At lower C_6H_6 pressures the suitable loadings are found to be 1 $\text{Mo}(\text{CO})_6$ and 25 C_6H_6 per unit cell and the corresponding sorption energies are found to be -7.0 and -10.6 kcal/mol, respectively. The distribution of

positions occupied by $\text{Mo}(\text{CO})_6$ and C_6H_6 is large. The absence of well-defined sorption sites indicates that the net potential surface accessible to the molecules is fairly uniform, a finding that is again consistent with the inability to locate the C_6H_6 sorbate in FAU by neutron diffraction.⁶² These results are in close agreement with the isotropic behavior observed from DRIFTS experiments. In addition, a recent Molecular Dynamics (MD) study concerning the behavior of benzene in FAU reveals that the sorbate is highly mobile at 300 K.²⁴

Na_{56}FAU ($n = 56$; $\text{Si}/\text{Al} = 2.49$). In the host lattice, the extraframework Na^+ cations are assumed to be located in site SII (32/32 Na^+) and in site SI' (24/32 Na^+). From accurate starting pressure values, the GCMC simulations provide loadings in reasonable agreement with the experimental values used in the DRIFTS experiments, 1 or 2 $\text{Mo}(\text{CO})_6$ and 30 C_6H_6 per unit cell, respectively. At high C_6H_6 pressures, the corresponding sorption energy is found to be -10 kcal/mol for $\text{Mo}(\text{CO})_6$ and -11 (window) and -19 kcal mol⁻¹ (cation) for C_6H_6 , respectively. It should be noted that similar energy values are reproduced for C_6H_6 during the simulation of the sorption of C_6H_6 alone.²³ The distribution of positions occupied by $\text{Mo}(\text{CO})_6$ according to the -11 kcal/mol energy is located within the cavity, whereas C_6H_6 molecules lie in the same cavity facially coordinated to the SII cations (-19 kcal/mol) or centered in the window (-11 kcal/mol). The presence of C_6H_6 molecules in the porous voids stabilizes the $\text{Mo}(\text{CO})_6$ location within the supercage rather than in the window as predicted by the MC simulations of the sorption of $\text{Mo}(\text{CO})_6$ alone.³⁷ It should be noted that in the case of cosorption when the average $\text{Mo}(\text{CO})_6$ loading is more than 2 molecules per unit cell, some supercages are occupied by 2 $\text{Mo}(\text{CO})_6$. The sorption energies of the benzene occluded alone in Na_{56}FAU or cosorbed with $\text{Mo}(\text{CO})_6$ are analogous whereas the sorption energy of $\text{Mo}(\text{CO})_6$ at low coverage is found to be markedly lower than cosorbed with benzene at high coverage, -12 and -10 kcal/mol, respectively. The siting locations of the C_6H_6 and $\text{Mo}(\text{CO})_6$ molecules are in good agreement with the DRIFTS data and the spectral changes observed in the $\nu(\text{CO})$ region reflects the $\text{Mo}(\text{CO})_6$ siting location change during the cosorption of benzene into the Na_{56}FAU zeolite.

Na_{96}FAU ($n = 96$; $\text{Si}/\text{Al} = 1$). In the host lattice, the extraframework cations are assumed to be located in site SI (16/16 Na^+), in site SII (32/32 Na^+), and in site SIII (48/48 Na^+). From accurate starting pressure values, the GCMC simulations provide a loading, corresponding to the sorption of 38 C_6H_6 per unit cell. There is no cosorption of $\text{Mo}(\text{CO})_6$ in the presence of benzene after equilibration of the system. The corresponding sorption energies are found to be -12 and -17 kcal/mol for C_6H_6 . The C_6H_6 molecules are facially coordinated to the SII and SIII cations in the supercage (-17 kcal mol⁻¹) or in the vicinity of the windows (-12 kcal mol⁻¹). Analogous energy values concerning the sorption of C_6H_6 in Na_{96}FAU were reported earlier.²¹ The sorption energy of $\text{Mo}(\text{CO})_6$ occluded alone in Na_{96}FAU at constant coverage was found previously to be -9 kcal/mol.³⁷ Before the saturation of the porous volume by the C_6H_6 molecules, the occluded $\text{Mo}(\text{CO})_6$ molecules observed during the DRIFTS experiments (see above) are probably located in domains without any benzene molecule in close proximity.

Identification of the Reaction Products within the Zeolitic Porous Space. DRIFTS Investigations of the Intrazeolite Reactions between $\text{Mo}(\text{CO})_6$ and C_6H_6 in Na_nFAU ($n = 0, 56, 85, 96$). *FAU* ($\text{Si}/\text{Al} > 100$). During the thermal treatment, under 1 atmosphere of helium, of the (0.5 $\text{Mo}(\text{CO})_6$, 20 C_6H_6)-FAU loaded zeolite no significant changes were observed in

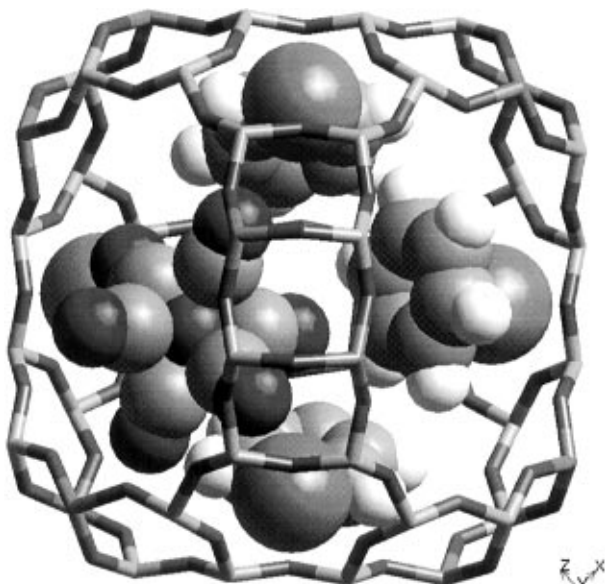


Figure 4. Predicted sorption sites of $\text{Mo}(\text{CO})_6$ and C_6H_6 in Na_{56}FAU (1 $\text{Mo}(\text{CO})_6$, 30 C_6H_6 /unit cell). The α -cage of zeolite Na_{56}FAU . The black and shaded cylinders represent O and Si/Al atoms of the zeolite framework, respectively. The shaded and white spheres represent C and H atoms of C_6H_6 , respectively. The large shaded spheres represent Na^+ ; the medium black and shaded spheres represent O and C atoms of $\text{Mo}(\text{CO})_6$, respectively.

the shapes of the DRIFTS spectra except the progressive disappearance of the intense band assigned to the ν_6 (CO) mode of $\text{Mo}(\text{CO})_6$ (Figure 5).³⁶

The disappearance of the ν_6 (CO) band corresponds to the desorption of $\text{Mo}(\text{CO})_6$ upon thermolysis before any reaction in the void space of the FAU zeolite. At 500 K, only C_6H_6 was detected in the internal volume of the zeolite. The $\text{Mo}(\text{CO})_6$ departure from the zeolite framework to the gas phase was controlled by IR absorption spectroscopy.

Na_{56}FAU ($n = 56$; Si/Al = 2.49). During the thermal treatment of the (2 $\text{Mo}(\text{CO})_6$, 30 C_6H_6)- Na_{56}FAU loaded zeolite, heating above 320 K again causes a dramatic change in the $\nu(\text{CO})$ set of bands whereas the C_6H_6 set of bands remains unaffected in the experimental [273–500 K] temperature range. The transformation appears to go to completion at 423 K over less than 0.5 h in the experimental conditions (Figure 6).

After subtraction from the resulting DRIFTS pattern of the DRIFTS bands of benzene the new $\nu(\text{CO})$ set of bands are found to be analogous to those observed for $\text{Mo}(\text{CO})_3(\eta^6\text{-C}_6\text{H}_6)$ occluded alone in Na_{56}FAU . It should be noted that the zeolite was loaded with $\text{Mo}(\text{CO})_3(\eta^6\text{-C}_6\text{H}_6)$ through immersion into the pentane solution and subsequent evaporation of the solvent because of the poor vapor pressure of the organometallic compound which does not allow any vapor phase transfer into the zeolite at room temperature.

The three $\nu(\text{CO})$ bands observed at 1948, 1857 and 1832 cm^{-1} (Table 2) do not correspond to any intrazeolite $\text{Mo}(\text{CO})_n$ ($n = 3, 4, 5$) subcarbonyl species.^{12,27,28,34,36} The three $\nu(\text{CO})$ bands derived from the A_1 and E modes of the $\text{Mo}(\text{CO})_3(\eta^6\text{-C}_6\text{H}_6)$ free molecule and indicate that the local symmetry is low in the sorption site. In practice one finds that the reaction of 2 $\text{Mo}(\text{CO})_6$ with 30 C_6H_6 in Na_{56}FAU cleanly yields as a product $\text{Mo}(\text{CO})_3(\eta^6\text{-C}_6\text{H}_6)$ according to the following intrazeolitic reaction.

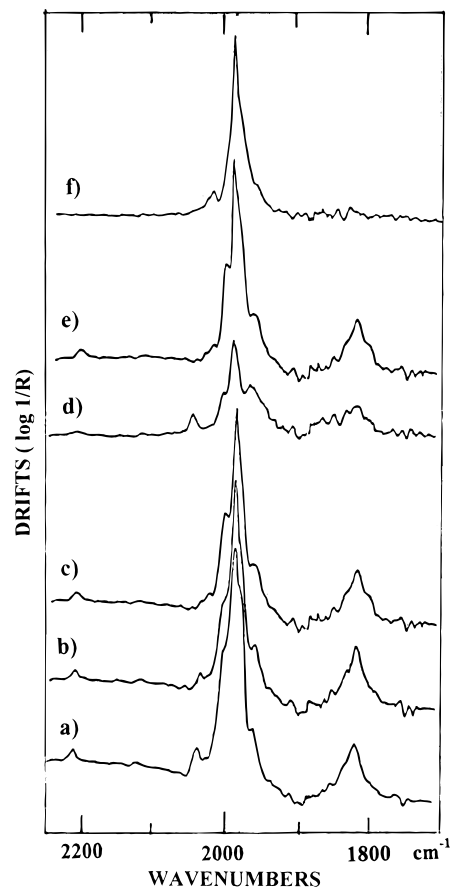
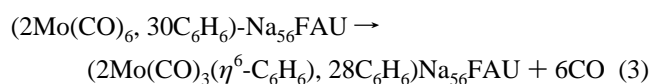
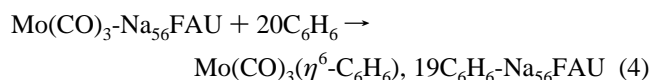


Figure 5. DRIFTS spectra in the $\nu(\text{CO})$ fundamental and $\gamma(\text{C-H})$ combination modes region during the thermal treatment of $\text{Mo}(\text{CO})_6$ and C_6H_6 cosorbed in FAU: (a) 0.2 $\text{Mo}(\text{CO})_6$, 25 C_6H_6 /unit cell (290 K); (b) a (360 K); (c) a (383 K); (d) a (433 K); (e) d (after cooling to 290 K); (f) spectrum e after subtraction of the C_6H_6 spectrum (290 K) equivalent to the $\text{Mo}(\text{CO})_6$ spectrum.

This intrazeolitically generated complex can be considered to form by capping the tricarbonyl moiety with the benzene ligand. Identical DRIFTS results are observed when an excess of benzene is introduced into the cell after partial decarbonylation reaction under thermolysis at 440 K. The intrazeolitic reaction of the subcarbonyl $\text{Mo}(\text{CO})_3\text{-Na}_{56}\text{FAU}$ with C_6H_6 yields as a product $\text{Mo}(\text{CO})_3(\eta^6\text{-C}_6\text{H}_6)$ according to the following intrazeolitic reaction.



No attempt to obtain quantitative kinetic information about the intrazeolitic reaction between $\text{Mo}(\text{CO})_6$ and C_6H_6 in Na_{56}FAU has been undertaken yet. Indeed, the main difficulty is to define and appreciate the “zero” time of the thermal activation with the heating set-up used. However, the reaction rate is found to be strongly dependent on the extent of loading of $\text{Mo}(\text{CO})_6$ and C_6H_6 and on the CO gas pressure. The effects of these parameters on intrazeolitic organometallic reaction rates have been quantitatively evaluated recently in the case of the reaction between $\text{Mo}(\text{CO})_6$ and trimethylphosphine in Na_{56}FAU .⁴² The general trends of the present work corroborate the quantitative kinetic data related to the later reaction. Particularly, after an equilibrium period (300 K), at low and quite constant $\text{Mo}(\text{CO})_6$

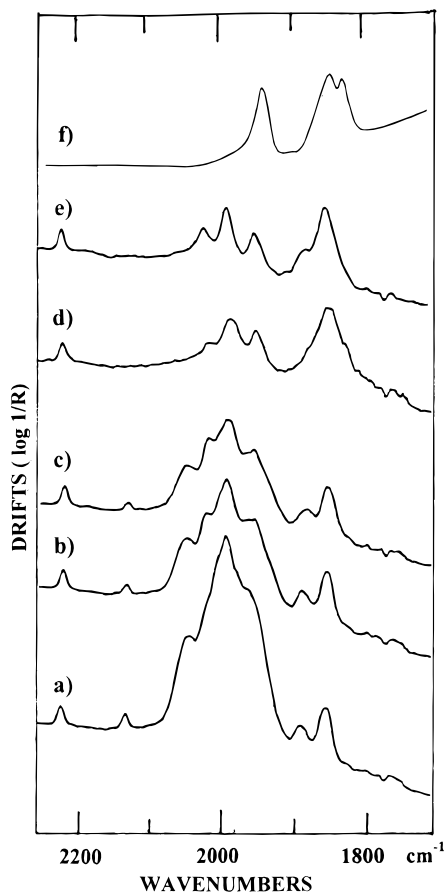


Figure 6. DRIFTS spectra in the $\nu(\text{CO})$ fundamental and $\gamma(\text{C-H})$ combination modes region during the thermal treatment of $\text{Mo}(\text{CO})_6$ and C_6H_6 cosorbed in Na_{56}FAU : (a) 0.2 $\text{Mo}(\text{CO})_6$, 25 C_6H_6 /unit cell (290 K); (b) a (320 K); (c) a (350 K); (d) a (423 K); (e) d (after cooling to 290 K); (f) spectrum e after subtraction of the C_6H_6 spectrum (290 K) equivalent to the $\text{Mo}(\text{CO})_3(\eta^6\text{-C}_6\text{H}_6)$ spectrum.

coverage, the reaction rate (400 K) increases slightly with increasing C_6H_6 loading in the experimental range (15–30 C_6H_6 /unit cell). Whereas at constant C_6H_6 coverage, the reaction rate remains approximately constant with increasing $\text{Mo}(\text{CO})_6$ loading over the range 0.02–1 $\text{Mo}(\text{CO})_6$ /unit cell. Then, the reaction rate shows a significant decrease at higher $\text{Mo}(\text{CO})_6$ loading. In addition, under dynamic vacuum the reaction appears faster than under static helium atmosphere. The amount of CO released during the reaction may be sufficient to decrease the rate substantially.

$\text{Na}_{85,96}\text{FAU}$ ($n = 85, 96$; $\text{Si}/\text{Al} = 1.26, 1$). When $\text{Mo}(\text{CO})_6$ was introduced at a relatively low temperature into the $\text{Na}_{85}\text{-FAU}$ zeolite, the carbonyl species entrapped in the zeolite framework was the intact $\text{Mo}(\text{CO})_6$ molecule. Indeed, no prominent infrared band was detected below 1900 cm^{-1} when the loading was carried out below 285 K. The DRIFTS spectra indicates no significant frequency shifts and relative intensity changes of the $\nu(\text{CO})$ modes upon cosorption of benzene. Heating above 300 K caused a dramatic change in the DRIFTS patterns (Figure 7).

After subtraction from the DRIFTS pattern of the benzene spectrum in Na_{85}FAU , the resulting $\nu(\text{CO})$ set of bands exhibits clearly the spectral characteristics of several anchored subcarbonyls species ($\text{Mo}(\text{CO})_x$, $x = 3-6$).³⁶ Near 500 K a two line spectrum is predominantly observed at 1912 and 1775–1750 cm^{-1} . This set of $\nu(\text{CO})$ bands was attributed previously to the intrazeolitic $\text{Mo}(\text{CO})_3\text{-Na}_{85}\text{FAU}$ species.^{27,28,34} The DRIFTS experiments provide no evidence of the intrazeolitic $\text{Mo}(\text{CO})_3(\eta^6\text{-C}_6\text{H}_6)\text{-Na}_{85}\text{FAU}$ species. In addition, heating above 500

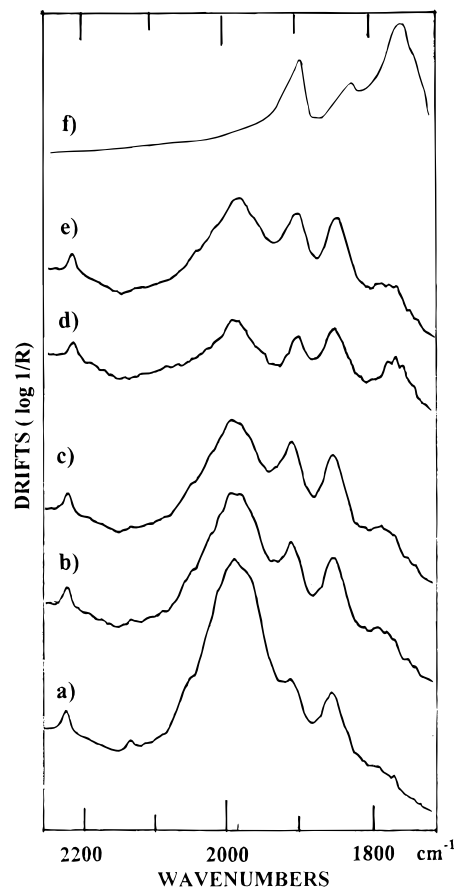


Figure 7. DRIFTS spectra in the $\nu(\text{CO})$ fundamental and $\gamma(\text{C-H})$ combination modes region during the thermal treatment of $\text{Mo}(\text{CO})_6$ and C_6H_6 cosorbed in Na_{85}FAU : (a) 0.2 $\text{Mo}(\text{CO})_6$, 25 C_6H_6 /unit cell (290 K); (b) a (320 K); (c) a (350 K); (d) a (500 K); (e) d (after cooling to 290 K); (f) spectrum e after subtraction of the C_6H_6 spectrum (290 K) equivalent to the $\text{Mo}(\text{CO})_3(\text{O}_2)_3$ spectrum.

K provokes the one step decomposition of $\text{Mo}(\text{CO})_3$ before any reaction with the benzene molecules. It should be noted that all DRIFTS results are found to be analogous with the $\text{Na}_{96}\text{-FAU}$ zeolite.

Energetics and Sorption Sites of the Reaction Products in the Zeolitic Porous Space. Monte Carlo Simulations of the Sorption of $\text{Mo}(\text{CO})_3(\eta^6\text{-C}_6\text{H}_6)$ and the Cosorption of $\text{Mo}(\text{CO})_3(\eta^6\text{-C}_6\text{H}_6)$ and C_6H_6 into Na_nFAU Zeolite Hosts ($n = 0, 56, 96$). The DRIFTS spectroscopic results are supported by both Canonical Monte Carlo (MC) at fixed loading and Grand Canonical Monte Carlo (GCMC) simulations at fixed pressures. The pressure values were adjusted to approximately mimic the experimental coverages. The conditions of the simulations have been given in the Experimental Section. The potential parameters and charges used for the MC simulations of the host-guest interactions are summarized in Table 1.

FAU ($n = 0$). The prediction of the $\text{Mo}(\text{CO})_3(\eta^6\text{-C}_6\text{H}_6)$ sorption and $\text{Mo}(\text{CO})_3(\eta^6\text{-C}_6\text{H}_6)\text{-C}_6\text{H}_6$ cosorption was carried out at 300 K and at fixed pressures. In the presence or in absence of C_6H_6 , the distribution of positions occupied by $\text{Mo}(\text{CO})_3(\eta^6\text{-C}_6\text{H}_6)$, in the vicinity of the window, is found to be large. The absence of well-defined sorption sites indicates that the net potential surfaces accessible to the molecules are fairly uniform. These results are consistent with the isotropic behavior of $\text{Mo}(\text{CO})_3(\eta^6\text{-C}_6\text{H}_6)$ in FAU observed from DRIFTS experiments. No further investigation has been undertaken yet, because this subject falls beyond the scope of this work. Indeed no intrazeolitic reaction between $\text{Mo}(\text{CO})_6$ and C_6H_6 is detected before the desorption of $\text{Mo}(\text{CO})_6$ (see above).

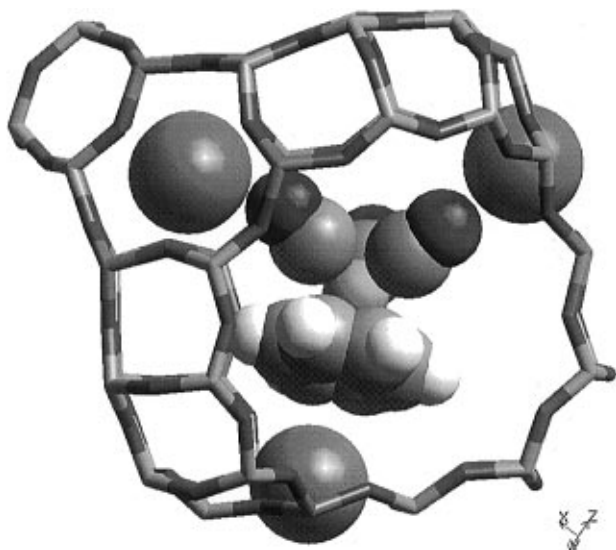


Figure 8. Probability density of $\text{Mo}(\text{CO})_3(\eta^6\text{-C}_6\text{H}_6)$ in Na_{56}FAU at low coverage (1 $\text{Mo}(\text{CO})_3(\eta^6\text{-C}_6\text{H}_6)$ /unit cell). A α -cage of zeolite Na_{56}FAU , the gray regions is where the sorbate center of mass is localized with 90% probability. The black and shaded cylinders represent O and Si/Al atoms of the zeolite framework, respectively. The shaded and white spheres represent the C and H atoms of C_6H_6 , respectively. The large shaded spheres represent Na^+ ; the medium black and shaded spheres represent O and C atoms of $\text{Mo}(\text{CO})_6$, respectively.

Na_{56}FAU ($n = 56$; Si/Al = 2.49). Firstly, the MC simulations of the sorption of $\text{Mo}(\text{CO})_3(\eta^6\text{-C}_6\text{H}_6)$ into Na_{56}FAU were carried out at 300 K and at a fixed loading. In this case the sorbate-sorbate interactions do not take place. The $\text{Mo}(\text{CO})_3(\eta^6\text{-C}_6\text{H}_6)$ molecule lies inside the supercage, the C_6H_6 moiety is facially coordinated to the SII Na^+ cation. However, 95% of the center of mass sampled during the simulations are located within an isosurface of the probability density of the molecule. This isosurface is shown in the plane of the Figure 8, the three lobes are oriented to the three remaining SII cations of the supercage, respectively. They represent the equal probability for each CO ligand to be in close proximity of a SII cation.

The prediction of sorption of $\text{Mo}(\text{CO})_3(\eta^6\text{-C}_6\text{H}_6)$ at higher filling was carried out at constant pressure. The average calculated loading corresponding to the filling of the voids were found to be 19 $\text{Mo}(\text{CO})_3(\eta^6\text{-C}_6\text{H}_6)$ per unit cell. The contoured regions of the distribution of positions of the center of mass provide clear evidence of two types of sorption sites. The first one corresponds to the SII Na^+ facially coordinated C_6H_6 moiety and the second one to the C_6H_6 moiety centered in the 12-ring window. The ratio of the population of the sites depends on the filling, particularly at high loading the confinement of the molecules in the porous void constrains the molecules to reside preferentially near the windows through intermolecular contacts. This sorption model appears to be in reasonable agreement with the previous and present IR spectroscopic data concerning $\text{Mo}(\text{CO})_3(\eta^6\text{-C}_6\text{H}_6)$ as well as parent complexes sorbed alone. Particularly, the set of three $\nu(\text{CO})$ bands corresponds to a $\text{Mo}(\text{CO})_3(\eta^6\text{-C}_6\text{H}_6)$ molecule sitting in a site with low local symmetry. However, the $\nu(\text{CO})$ stretching frequencies are shifted toward lower energies by about 60 cm^{-1} compared to the respective solution phase values. In addition, the supplementary splittings or broadenings of the bands, which occur at higher coverage, can be attributed to the two different types of sorption sites and vibrational intermolecular couplings.

The GCMC simulations of the $\text{Mo}(\text{CO})_3(\eta^6\text{-C}_6\text{H}_6)\text{-C}_6\text{H}_6$ cosorption are directly related to the *in situ* DRIFTS study of the intrazeolitic reaction between $\text{Mo}(\text{CO})_6$ and C_6H_6 cosorbed in Na_{56}FAU . From accurate starting pressure values, the GCMC

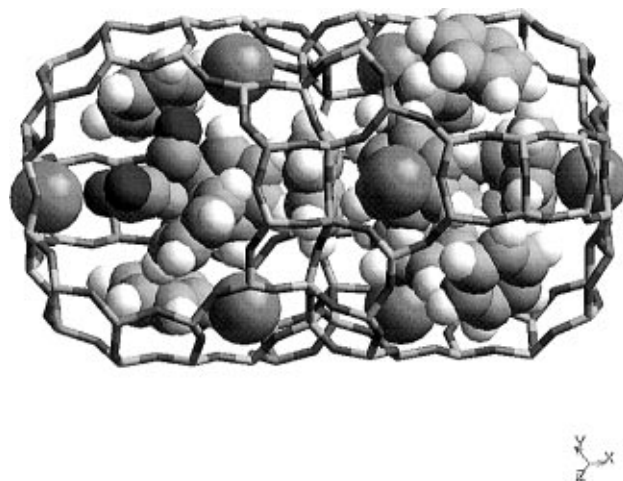


Figure 9. Predicted sites of $\text{Mo}(\text{CO})_3(\eta^6\text{-C}_6\text{H}_6)$ and C_6H_6 cosorbed in Na_{56}FAU (1 $\text{Mo}(\text{CO})_3(\eta^6\text{-C}_6\text{H}_6)$, 30 C_6H_6 /unit cell). Two α -cages of zeolite Na_{56}FAU and the interconnecting 12-ring window of diameter 8 Å. The black and shaded cylinders represent O and Si/Al atoms of the zeolite framework, respectively. The shaded and white spheres represent the C and H atoms of C_6H_6 , respectively. The large shaded spheres represent Na^+ ; the medium black and shaded spheres represent O and C atoms of $\text{Mo}(\text{CO})_6$, respectively.

simulations provide loadings in reasonable agreement with the experimental values used in the DRIFTS experiments, 2 $\text{Mo}(\text{CO})_6$ and 28 C_6H_6 per unit cell, respectively. The distribution of positions occupied by $\text{Mo}(\text{CO})_3(\eta^6\text{-C}_6\text{H}_6)$ according to the -21 kcal/mol energy is located within the cavity, whereas the C_6H_6 molecules are facially coordinated to the SII cations in the supercage (-19 kcal) or centered in the window (-11 kcal). The C_6H_6 moiety of the $\text{Mo}(\text{CO})_3(\eta^6\text{-C}_6\text{H}_6)$ molecule is facially coordinated to the SII Na^+ cation (Figure 9).

The presence of C_6H_6 molecules in the void space does not markedly modify the siting site preference predicted by the MC simulations of the sorption of the $\text{Mo}(\text{CO})_3(\eta^6\text{-C}_6\text{H}_6)$ molecule alone. The sorption energies of the benzene sorbed alone in Na_{56}FAU or cosorbed with $\text{Mo}(\text{CO})_3(\eta^6\text{-C}_6\text{H}_6)$ are analogous, whereas the energy of $\text{Mo}(\text{CO})_3(\eta^6\text{-C}_6\text{H}_6)$ sorbed alone at low coverage is found to be slightly higher than cosorbed with benzene at high coverage, -20 and -21 kcal/mol , respectively. The siting locations of the C_6H_6 and $\text{Mo}(\text{CO})_3(\eta^6\text{-C}_6\text{H}_6)$ molecules appear to be in close agreement with the DRIFTS data. Particularly, the weak changes observed between the $\nu(\text{CO})$ sets, reflect an analogous siting location for $\text{Mo}(\text{CO})_3(\eta^6\text{-C}_6\text{H}_6)$ sorbed alone or cosorbed with C_6H_6 in the Na_{56}FAU zeolite.

Na_{96}FAU ($n = 96$; Si/Al = 1). Firstly, the MC simulations of the sorption of $\text{Mo}(\text{CO})_3(\eta^6\text{-C}_6\text{H}_6)$ into Na_{96}FAU were carried out at 300 K at fixed loading. The lowest energy site (-1 kcal) for the $\text{Mo}(\text{CO})_3(\eta^6\text{-C}_6\text{H}_6)$ sorption was found to be in the vicinity of the window, the C_6H_6 moiety being centered in the 12-membered ring and the O atoms of the $\text{Mo}(\text{CO})_3$ moiety in close contact with the SII and SIII Na^+ cations of one supercage.

The prediction of sorption of $\text{Mo}(\text{CO})_3(\eta^6\text{-C}_6\text{H}_6)$ at higher filling was carried out at constant pressure. The average calculated loading corresponding to the filling of the voids was found to be 18 $\text{Mo}(\text{CO})_3(\eta^6\text{-C}_6\text{H}_6)$ per unit cell. The contoured regions of the distribution of positions of the center of mass provide clear evidence of three types of sorption site. According to the plot, number of configurations versus the energy, the sorption energy values are found to be -24 , -31 , and -39 kcal mol^{-1} . The first one corresponds to the SII Na^+ facially coordinated C_6H_6 moiety, the second one to the C_6H_6 moiety centered in the 12-ring window and the last one to a molecule

with the C₆H₆ moiety perpendicular to the window plane. The ratio of the population of the sites depends on the filling. Indeed, at high loading the confinement of the molecules in the porous void constrains the molecules to reside in unusual sites through intermolecular contacts.

From accurate starting pressure values, in agreement with the experimental values, there is no cosorption of Mo(CO)₃-(η^6 -C₆H₆) in the presence of benzene in Na₈₅FAU after equilibration of the system. The simulations of the cosorption exhibit striking analogy with the simulations of the C₆H₆ sorption into Na₈₅FAU. Nevertheless, during the Mo(CO)₆-C₆H₆ cosorption before the saturation of the porous volume by the C₆H₆ molecules, the occluded Mo(CO)₆ molecules are probably located in domains without any benzene molecule in close proximity. Consequently, upon thermal treatment, under gentle warming, several subcarbonyl species are generated and immobilized in the zeolite framework as observed previously for the thermolysis of occluded Mo(CO)₆ in Na₈₅FAU.³⁴⁻³⁶ Under more drastic conditions (400 K) the composition of the major species was found to be Mo(CO)₃.³⁴⁻³⁶ So, using accurate atom-atom potential values taking into account the Mo atom (Table 1), the MC simulations provide a reasonable picture of the anchoring site for the Mo(CO)₃ subcarbonyl species in the void space of the Na₉₆FAU. The Mo(CO)₃ appears located in the vicinity of the window, the three shortest O(zeolite)---Mo distances are found to be in the [2.2-3.4] Å, whereas the closest O(CO)---Na⁺ contacts are found to be about 3 Å. The model considers the immobilization of the tricarbonyl molybdenum moiety on the O atom of the zeolite framework over a vacant four-ring site in the vicinity of the window and involves interactions with cations through the oxygen end of the carbonyls to the Na⁺ cations. The EXAFS experiments for Mo(CO)₃ immobilized in faujasitic zeolites provide strong support concerning the structure analysis.³⁵ The best fit carbonyl and oxygen coordination numbers yield the stoichiometry (zeolite)-O_{2,3}---Mo(CO)₃ with a dramatic decrease in the Mo-CO and Mo-C-O bond lengths compared to those in the parent Mo(CO)₆ loaded zeolite. In addition, it was shown that the Mo-CO and Mo---O(zeolite) bond lengths are found to parallel the Lewis basicity of the O atoms of the zeolite. The structural parameters obtained through the present MC simulations are found to be in reasonable agreement with the earlier EXAFS data.³⁵ An analogy between the internal surface of the void space of the zeolite (zeolate ligand) and crown ether ligands has been proposed previously, particularly through the basicity of the oxygen framework atoms.¹²

Reaction Pathways between Mo(CO)₆ and C₆H₆ within the Void Space of Zeolitic Faujasites Na_nFAU (n = 0, 56, 85, 96). Conclusions. Treatment of metal carbonyls such as Mo(CO)₆ with arenes such as C₆H₆ in solution may give arene metal carbonyl complexes.¹⁵ Irradiation with ultraviolet light assists the reaction, or it may be more effective to carry out the reaction in a high-boiling, coordinating solvent such as diglyme (CH₃OCH₂CH₂OCH₂CH₂OCH₃). The role of the coordinating solvent was found to accelerate the dissociation of Mo(CO)₆ which is found to be slow.

It is known that Mo(CO)₆ can react thermally in the void space of zeolites in the absence of added reagents.^{18,34-36} From previous experiments including EXAFS, NMR, XPS, FTIR and chemical analysis results the main findings can be summarized as follows: The faujasitic zeolites with high aluminum content (Si/Al = 1, 1.26) promote an easy sequential decomposition of Mo(CO)₆. The loss of three CO ligands of Mo(CO)₆ forms a moiety in which the three coordination sites thus made vacant are occupied by framework oxygens of the four-rings acting as

a zeolate ligand.¹² The subcarbonyl species are stabilized through the significant Lewis basicity (electron density) of the framework oxygens.^{28,35} The basicity of the oxygen, measured through the charge density, decreases concomitantly with the aluminum content of the zeolite framework. The Na₅₆FAU framework (Si/Al = 2.5) reduces the stabilization of the subcarbonyl species and increases the intrazeolite decomposition temperature of Mo(CO)₆.³⁶ The Mo(CO)₆ thermal behavior in siliceous faujasite FAU (Si/Al = 100) is found to be analogous to that observed in polyether solvents where no discrete subcarbonyl species are detected. In summary, a significant basicity of the framework oxygens prevent the recombination reactions of the subcarbonyl species with CO inside the void space.

An extensive quantitative kinetic study of the thermal reaction between Mo(CO)₆ and trimethyl phosphine PMe₃ encapsulated in Na₅₆FAU has been recently reported.⁴² The effects of PMe₃, Mo(CO)₆ loadings and CO pressure on the rate of the substitution reactions to form Mo(CO)₄(PMe₃)₂ have been evaluated. The substitution reactions of Mo(CO)₆ with PMe₃ within the void space of the Na₅₆FAU host proceed by pseudo-first-order dissociative and associative processes. Analogous trends have been found here. Dissociative substitution of Mo(CO)₆ by C₆H₆ is accelerated through evacuation of CO under vacuum or retarded to a significant extent by increased CO pressure as Mo(CO)₆ and C₆H₆ loading. The reactions between Mo(CO)₆ and C₆H₆ to form Mo(CO)₃(η^6 -C₆H₆) within the void space of Na₅₆-FAU (Si/Al = 2.5) occur at lower temperature and are faster than the corresponding reactions in homogeneous solution. However, the present experiments point out the important role of the nature of the faujasitic zeolite towards the substitution reactions under study. Particularly, the aluminum content of the zeolite appears to be a crucial factor of the chemical behavior inside the void space. In FAU (Si/Al = 100) no reaction occurs between Mo(CO)₆ and C₆H₆ under thermal activation limited by the desorption of Mo(CO)₆ whereas in Na₈₅₋₉₆FAU, Mo(CO)₆ reacts thermally like in the absence of added reagent to form anchored subcarbonyl Mo(CO)_n (n = 5, 4, 3) species. It should be noted that the nature of the counterbalancing charge cations is an additional factor of the chemical behavior within the void space.²⁸ Earlier papers related to arenes or Mo(CO)₆ sorbed alone in faujasitic zeolites and the present work devoted to the cosorption provide theoretical and experimental supports through the siting location and dynamic behaviors of the C₆H₆ and Mo(CO)₆ molecules in faujasitic zeolites, thus a coherent interpretation of the chemical behavior between Mo(CO)₆ and C₆H₆ inside the void space of the faujasitic zeolites can be proposed.

In siliceous FAU, the Mo(CO)₆ and C₆H₆ molecules are not located at specific sites, they are randomly distributed in the void space. The dynamic behavior of benzene molecules sorbed alone is largely dominated by intracavity motions at room temperature. At 400 K, the benzene molecule is considerably more mobile and exhibits cage-to-cage diffusion. After cosorption in FAU, the motions of Mo(CO)₆ and C₆H₆ approach the rapid isotropic limit of liquids. The chemical behavior between Mo(CO)₆ and C₆H₆ is found to be analogous to that observed in solution.

In Na₅₆FAU, the benzene molecule is facially located to the SII sodium cation or in the plane of the window.¹⁶ Dynamic studies indicate intracavity "cartwheel" and "skateboard" hopping mechanisms whereas the diffusion is determined simply by the site-to-window hopping rate. The kinetic motions are found to be slower than in the siliceous analog. Similar trends have been predicted for Mo(CO)₆. In the presence of Mo(CO)₆,

the C_6H_6 molecules are predicted to be facially located to the SII cation or in the window as determined for C_6H_6 sorbed alone, whereas $Mo(CO)_6$ at low coverage is held within the supercage in close proximity of benzene molecules. The diffusion of the reagents are probably hindered at higher coverages. The enhancement of the reaction rate at relatively low coverage can be attributed to (i) the close proximity of the reagents in the supercage, (ii) the intense electrostatic field gradient, and (iii) the concerted mechanism of the dissociation of $Mo(CO)_6$ with the coordination of framework oxygen atoms and slippage of the $Mo(CO)_3$ group to the arene molecule. The substitutional affinity of the grafted $Mo(CO)_3$ depend both on the basicity of the framework oxygen atoms and on the nature of the entering arene.⁶³ The slippage probably proceeds via $Mo(CO)_3(\eta^{2y}-C_6H_6)(O_z)_{3-y}$ ($y = 1, 2$) intermediates without any displacement of the C_6H_6 molecule from his site. Indeed, after the reaction, the $Mo(CO)_3(\eta^6-C_6H_6)$ species is predominantly anchored via the facially oriented C_6H_6 ligand to the SII cation.

In $Na_{(85-96)}FAU$ zeolites, the C_6H_6 sorbed alone is predicted to be facially coordinated to the SII or SIII cations whereas at low coverage the $Mo(CO)_6$ molecule sorbed alone is predominantly located within the supercage. In the presence of C_6H_6 no stable sorption site for $Mo(CO)_6$ is predicted in the same

cavity. The high basicity of the framework oxygen atoms stabilized the subcarbonyl $Mo(CO)_3$ species through the coordination with the four-ring oxygen atoms. Even coordinated to the zeolite framework, the $Mo(CO)_3$ group remains mobile;³⁸ however, the exchange from the framework oxygen atoms to the arene is not effective.

The activity of the anchored $Mo(CO)_n$ ($n = 5, 4, 3$) species within the void space of faujasitic zeolites as active species to hydrogenation and isomerization of dienes may be due to their abilities to coordinate substrates at the expense of $Mo-O_z$ bonds. In addition to the molecular sieves properties, the role of the support is crucial particularly through the basicity of the framework oxygen atoms and the nature of the extraframework cations. The aluminum content and the extraframework cation are means to optimize the faujasitic zeolite syntheses in view of the expected catalytic properties. However, the availability of open coordination sites does not appear as the rate-determining step of the catalytic reaction, the catalytic pathway includes the sequential complexation, functionalization and liberation of unsaturated hydrocarbons which constitute one of the most important reaction sequences in catalytic organometallic synthesis.

JA961115Z